original article

Histopathology and surgical anatomy of patients with primary hyperparathyroidism and calcium phosphate stones

Andrew E. Evan[1], James E. Lingeman[2], Fredric L. Coe[3], Nicole L. Miller[4], Sharon B. Bledsoe[1], Andre J. Sommer[5], James C. Williams[1], Youzhi Shao[1] and Elaine M. Worcester[3]

[1]Department of Anatomy and Cell Biology, Indiana University School of Medicine, Indianapolis, Indiana, USA; [2]International Kidney Stone Institute, Methodist Clarian Hospital, Indianapolis, Indiana, USA; [3]Department of Medicine, University of Chicago, Chicago, Illinois, USA; [4]Department of Urology, Vanderbilt University, Nashville, Tennessee, USA and [5]Department of Chemistry and Biochemistry, Miami University, Oxford, Ohio, USA

Using a combination of intra-operative digital photography and micro-biopsy we measured renal cortical and papillary changes in five patients with primary hyperparathyroidism and abundant calcium phosphate kidney stones. Major tissue changes were variable papillary flattening and retraction, dilation of the ducts of Bellini, and plugging with apatite deposits of the inner medullary collecting ducts and ducts of Bellini. Some of the papillae in two of the patients contained plentiful large interstitial deposits of Randall's plaque and where the deposits were most plentiful we found overgrowth of the attached stones. Hence, this disease combines features previously described in brushite stone formers – dilation, plugging of ducts and papillary deformity – with the interstitial plaque and stone overgrowth characteristic of routine idiopathic calcium oxalate stone formers, suggesting that these two patterns can coexist in a single patient.

Correspondence: *Andrew E. Evan, Department of Anatomy and Cell Biology, Indiana University School of Medicine, 635 Barnhill Drive, MS 5055S, Indianapolis IN 46223, USA. E-mail: evan@anatomy.iupui.edu*

Using a combination of intra-operative digital photography and micro-biopsy, we have described gross and histopathological renal papillary and cortical changes in patients with brushite,[1] apatite stones, and distal renal tubular acidosis (dRTA);[2] and patients with calcium oxalate (CaOx) stones from obesity bypass procedures,[3] cystinuria,[4] and idiopathic CaOx stones (ICSF).[3,5] In all but ICSF, we found (a) a mixture of inner medullary collecting duct (IMCD) and duct of Bellini (BD) plugging with apatite or, in the case of cystinuria, IMCD apatite and BD cystine crystals; (b) variable papillary flattening and atrophy; (c) interstitial fibrosis; and (d) epithelial cell loss. In ICSF, by contrast, we found only interstitial apatite deposits, the so-called Randall's plaque[6] with otherwise normal renal tissue. Of crucial importance, stones appear to grow on papillary surfaces of ICSF at sites of sub-urothelial plaque,[5,6] whereas such overgrowth was not found by us in any of the other aforementioned conditions.

Primary hyperparathyroidism (HPT) with stones spans a spectrum from CaOx to calcium phosphate (CaP) stones;[7,8] we would expect patients with HPT who form CaP stones to have a surgical anatomy and renal histopathology similar to those with brushite and apatite stone. However, to date this prediction has not been tested. We report here the surprising fact that among five patients with HPT and predominantly CaP stones, we found both IMCD crystal plugging with associated papillary injury, as well as abundant plaque with attached stones. This is the first disease instance thus far in which attached stones on plaque coexists with IMCD plugging.

RESULTS
Clinical information
All but one patient was female, and had formed multiple stones (Table 1). The stones from these patients that were available for analysis were predominantly CaP; however, for patient 1 we had only one stone that was analyzed as predominantly CaOx. Parathyroidectomy was performed on the day of, or within a few weeks after, percutaneous

Table 1 | Clinical characteristics of biopsied patients

Case	Sex	Age of first stone	Stones	ESWL	PNL	Total Procedures	Age at biopsy	Age at PTX	Duration of known ↑ serum Ca	Stone composition (%)		
										CaOx	HA/BR	Struvite
1	F	48	4/2	0	2/1	2/1	49	49	>3.5 years	67	33/0	0
2	M	52	5/?	1/?	2/1	5/?	53	53	<12 months	0	0/100	0
3[a]	F	29	11/7	0	3/1	13/5	34	34	5 years	28	34/38	0
4	F	30	3/2	1/1	1/1	4/2	37	37	2 years	7	43/50	0
5	F	33	3/1	0	1/1	3/1	34	34	3 months	21	65/0	14

BR, brushite; CaOx, calcium oxalate; ESWL, extra-corporeal shock wave lithotripsy before biopsy (total/biopsied kidney); HA, hydroxyapatite; PNL, percutaneous nephrolithotomy before biopsy (total/biopsied kidney); Procedures, ureteroscopy, laser lithotripsy, nephrectomy, ESWL, PNL (total/biopsied kidney); PTX, parathyroidectomy; Stones, total stones/stones from biopsied kidney; Stone composition, the net % including all analyzed stones.
[a]This case had nephrectomy 1.5 years before biopsy, for non-function.

Table 2 | Selected laboratory data for biopsied patients

Case	Collection period	Serum				24-h urine				
		Calcium (mg per 100 ml)	PTH (pg/ml)	Creat (mg per 100 ml)	EGFR (ml/min/1.73 m^2)	pH	Volume (l day^{-1})	Ca/Creat (mg/g)	SSCaOx	SSCaP
1	Pre-PTX	11.0	172	1.1	56	ND	ND	ND	ND	ND
	Post-PTX	9.3	76	1.2	51	5.58	1.32	107	4.4	0.14
2	Pre-PTX	12.2	233	0.8	107	6.90	2.41	174	7.5	2.4
	Post-PTX	9.8	ND	1	83	6.89	2.12	118	5.7	2.1
3	Pre-PTX	11.2	149	1.2	55	ND	ND	ND	ND	ND
	Post-PTX	ND	ND	ND	ND	8.54	0.94	11	1.2	0.1
4	Pre-PTX	10.8	188	0.9	75	5.65	1.92	261	11.9	1.1
	Post-PTX	9.4	25	ND	ND	5.97	1.28	75	7.1	0.8
5	Pre-PTX	11.3	143	1.5	42	ND	ND	ND	ND	ND
	Post-PTX	8.1	ND	1.7	37	5.93	1.53	88	5.4	0.6

Ca/Creat, ratio of urine calcium to creatinine concentrations from 24 h collections, normal value is up to 140 mg/g; Creat, creatinine; eGFR, MDRD-calculated glomerular filtration rate; post-PTX, post-parathyroidectomy; pre-PTX, pre-parathyroidectomy; PTH, parathyroid hormone; SS, supersaturation.
Serum and urine were not collected on the same days.

nephrolithotomy at which the renal biopsies reported here were obtained. Hypercalcemia had been present for months to years (Table 1), was of moderate degree (Table 2), and was accompanied by elevated serum PTH levels. Pre-parathyroidectomy 24-h urine studies were available in only two cases (Table 2) and showed the expected hypercalciuria. A parathyroid adenoma was found at surgery in all five patients and successfully removed. In four cases we were able to obtain postoperative serum calcium values (Table 2). Post-parathyroidectomy urine calcium values were obtained from all five patients and were normal, as were supersaturations with respect to CaOx and CaP. Urine pH, a principle determinant of CaP supersaturation, was not alkaline except in patients 2 and 3 (Table 2); the peak of the pH value in patient 3 indicates probable contamination with a urea-splitting organism, which was confirmed by high ammonia (53 mEq/day), and low magnesium (1.5 mg/day) and phosphate (0.114 g/day) levels. Notably, serum creatinine values were slightly elevated and estimated glomerular filtration rates reduced.

Table 1 presents the total number of stones found in each patient and the net percentage of CaOx, hydroxyapatite/brushite (HA/BR), and struvite for all analyzed stones. A further breakdown of the number of stones analyzed per patient and the composition of each stone is presented here.

Patient 1 had four stones analyzed with the following mineral compositions: 42% HA and 58% CaOx; 73% HA and 27% CaOx; 18% HA and 82% CaOx; 1% HA and 99% CaOx. Patient 2 had two stones analyzed with the following mineral compositions: 100% BR; 100% BR. Patient 3 had five stone analyzed with the following mineral compositions: 32% HA and 68% CaOx; 20% BR, 30% HA and 50% CaOx; 60% HA and 40% CaOx; 100% BR; 50% HA and 50% CaOx. Patient 4 had two stones analyzed with the following mineral compositions: 87% HA and 13% CaOx; 100% BR. Patient 5 had four stones analyzed with the following mineral compositions: 90% HA and 10 CaOx; 45% HA and 55% struvite; 37% HA and 63% CaOx; 89% HA and 11% CaOx.

Renal surgical pathology

Patient one displayed the least amount of papillary pathology (Figure 1a), consisting of scattered white Randall's plaque in amounts similar to those found in normal people, that is less than 1%.[9] Even so, two papillae of this same patient (Figure 1b) showed marked retraction, and markedly dilated BD with protruding crystal plugs. All the papillae of patients 2 and 3 (Figures 2 and 3) showed the advanced changes, retraction, BD dilation and plugging, that were seen in only some papillae of patient 1. In addition, these two patients had yellow plaque, the known gross morphological appearance of
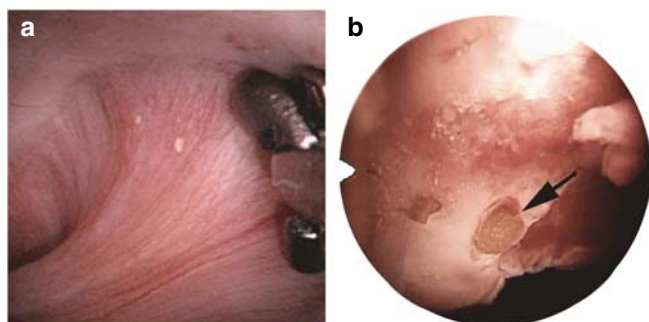
Figure 1 | Range of papillary pathology in one patient (patient 1). Most papillae were normal appearing (**a**) with small regions of Randall's plaque. Note the presence of biopsy forceps at upper right. Two papillae contained markedly dilated BD with crystalline plugging (**b**, arrow) and were retracted.
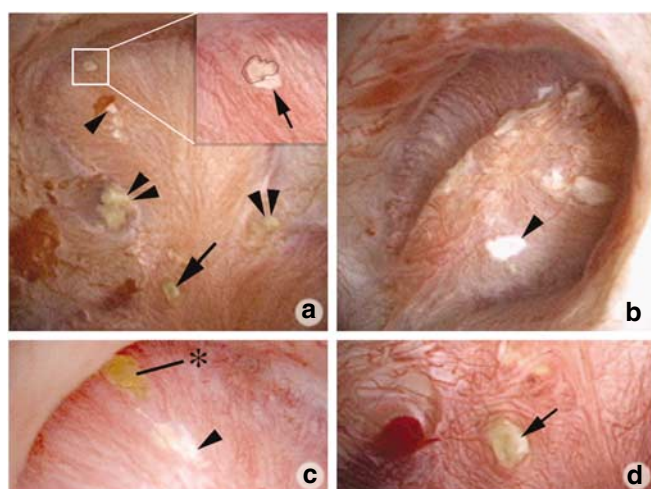

Figure 2 | Coexistence of attached stones and BD plugging on the same papillae (patient 2). (**a**) Areas of yellow plaque (IMCD crystal deposit, double arrowheads) and white interstitial (Randall's) plaque (single arrowhead) are found on one papilla. One dilated BD has a crystalline plug (arrow) protruding from its opening. A stone attached at an area of white plaque (within the white box) is magnified in the inset at the upper right; the stone is outlined within the inset by a black dotted overlay and the plaque border is indicated with an arrow. (**b**) Large areas of white plaque (single arrowhead) are evident on another papilla of this patient. (**c**) On another papilla a stone (asterisk) is attached to the papilla near an area of white plaque (single arrowhead). (**d**) On yet another papilla a dilated BD with plugging (arrow) is near the yellow plaque.

Figure 3 | Attached stone prior to, during, and after removal (patient 3). (**a**) An attached stone (asterisk) is near areas of yellow (double arrowhead) and white (single arrowhead) plaque. (**b**) The stone in panel (**a**) is being removed by a basket during percutaneous nephrolithotomy (asterisk); it was attached to an area of white plaque (single arrowhead) deep beneath the stone surface. This stone was also overlying a dilated BD (double arrows) and is adjacent to a large crystalline plug (small arrows) protruding from another dilated BD. (**c**) Light-microscopy image of the stone (2 mm) in panel (**b**), after removal. Many large CaOx dihydrate crystals (arrows) cover the urinary surface of the stone. (**d**) μCT analysis of the same stone reveals a mixture of apatite (white regions) and CaOx dihydrate (gray regions).

IMCD apatite plugging.[1] (Figures 2a and d and 3a and b). Large amounts of white (Randall's) plaque were also observed (Figure 2b and c), as were attached stones in some areas of white plaque (Figures 2a and c; 3a and b). Attached stones were on the same papillae in which BD were plugged with crystals (Figure 2a and c). Figure 3 shows an attached stone on a papilla obtained from patient 3 prior to removal (Figure 3a); during removal, exposing a region of white plaque deep within the site of stone attachment (Figure 3b); after removal (Figure 3c); and a micro-computed tomography (μCT) i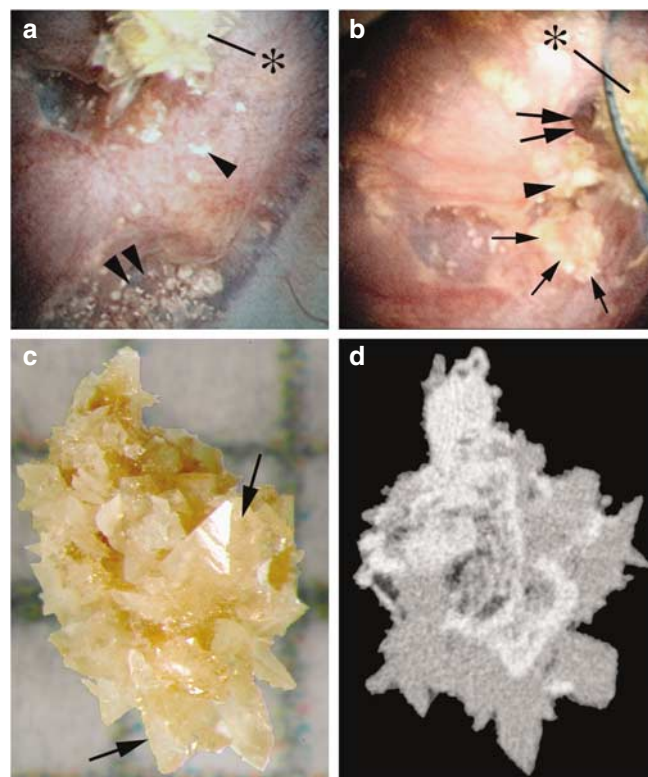mage of the same stone (Figure 3d). μCT analysis reveals the mineral composition of the stone to be mixed, the whitish areas being apatite and the gray areas CaOx dihydrate. Patients 5 and 4 displayed the most advanced changes (Figure 4). Papillae were flattened with numerous dilated BD (Figure 4a and b), occasionally with crystalline plugs (arrow). The visual impression that larger amounts of white plaque were present on the papillae of patients 2 and 3 than on the papillae of the other three patients was confirmed by digital imaging. The percent of papillary surface covered by white plaque in patients 2 and 3 exceeded that of the other three patients by over 10-fold (Table 3).

Histopathological findings

Patient 1, who had a predominantly CaOx stone admixed with 33% apatite, had a few, very large IMCD plugs (Figure 5a and b) with little plaque. Patient 3, who had brushite and apatite stones, showed presence of large amount of IMCD deposit on high-resolution CT and histopathology (Figure 5c and d) along with abundant plaque. Patient 2, who

also had brushite-containing stones, showed presence of a similar amount of IMCD plugging and abundant plaque (Figure 5e and f) as in patient 3; this patient, as noted, along with patient 2, had stones attached to plaque (Figure 2a and c). When found, by high-resolution CT and light microscopy, patients 4 and 5 (not illustrated) to have a moderate amount of BD plugging and dilation, but lacking abundant white plaque and attached stones.

Pathological changes were extreme in some areas (Figure 6a). Plugging of IMCD and BD with mineral led to loss of cells and interstitial fibrosis in patient 3. Very heavy deposits of Randall's plaque were observed in patient 2 (Figure 6b, Table 3), with the expected preservation of interstitial integrity. In patient 1 (Figure 6c), a single massive intra-tubular plug (center of panel), visualized by high-resolution CT in the lower left quadrant of the panel, led to total loss of epithelial cells. The mineral phase reaches to the surface of the basement membrane (lower right quadrant of panel). A ring of fibroblasts surrounds the plugged duct.

The number of IMCD and BD deposits per biopsy differed widely among our patients (Table 3). Three patients had mineral deposits (patients 1, 4, and 5) extending from the inner medulla through outer medulla to the cortex (Table 3). In the outer medulla of patient 5 (Figure 7a), deposits are in the outer medullary collecting ducts and extend into the cortical collecting ducts (Figure 7b). The same changes in patients 1 and 4 are not illustrated.

We determined the composition of intratubular deposits in all five papillary and three cortical and outer medullary sections using micro-Fourier transform infrared spectro-

meter; in every case, deposits were biological apatite (Figure 8). In the two cases (patients 2 and 3) with abundant interstitial plaque and attached stones, the mineral phase of the plaque was biological apatite (Figure 8).
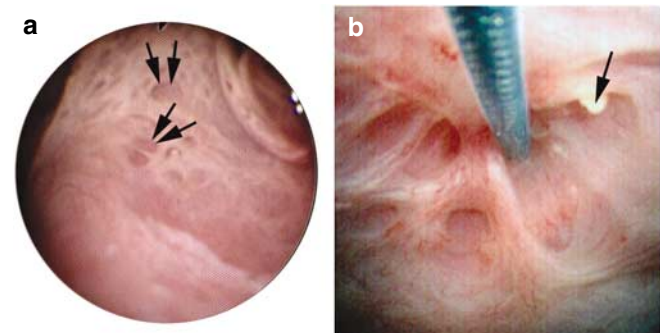

Figure 5 | Relative densities of IMCD deposits and interstitial plaque. μCT imaging (**a**, **c**, **e**) and histopathology (**b**, **d**, **f**). (**a**) Patient 1 had a few huge deposits (arrows) in IMCD by μCT analysis. (**b**) One of the large deposits (single arrow) in patient 1 is associated with loss of epithelium (decalcified light microscopic section, double arrow); Randall's plaque is not present. In patient 3 (**c**, **d**) and patient 2 (**e**, **f**), many IMCD deposits (arrows) are associated with Randall's plaque (arrowheads). Patients 4 and 5 had a moderate amount of IMCD deposits (not shown). Original magnification × 30 (**b**); × 150 (**d**, **f**). Panels (**d**) and (**f**) are Yasue staining images; panel (**b**) is an image of toluidine blue staining.

Figure 4 | Severe papillary changes. Patient 5 (**a**) and patient 4 (**b**). The most severe changes consisted of papillary retraction and flattening associated with numerous dilated BD (double arrows), some with crystalline plugs (arrow); white plaque is absent.
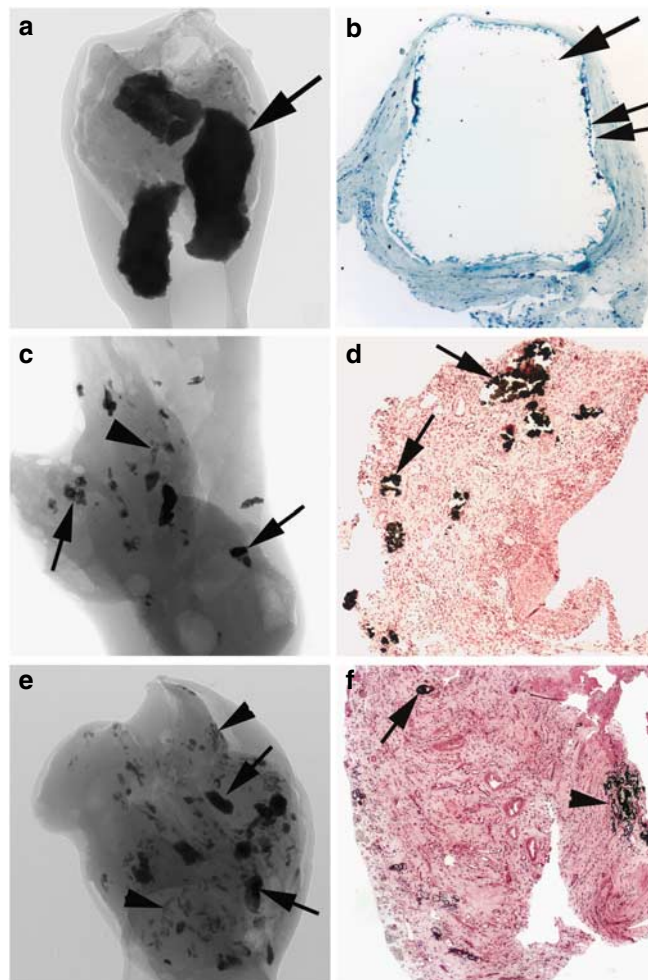
Table 3 | Summary of pathological changes

Patient	Papillary deformity (%)	White plaque (%)	Yellow plaque	Attached stones	IMCD/BD deposits	Cortical deposits
1	<50	0.28	Some	No	2 ± 1	Yes
2	>50	15.9	Some	Yes	25 ± 2	No
3	>50	2.8	Some	Yes	24 ± 3	No
4	>50	0.15	Some	No	10 ± 1	Yes
5	>50	0.17	Some	No	6 ± 1	Yes

BD, duct of Bellini; IMCD, inner medullary collecting duct; IMCD/BD deposits, number of individual intra-luminal deposits per square millimeter of tissue, ± s.e.m. Percent papillary deformity refers to the fraction of papillae visualized at the time of surgery with deformity; white plaque is expressed as percent of papillary surface covered by white plaque; IMCD, previously published value for mean plaque coverage measured in four patients with no stone was 0.5%.[9]
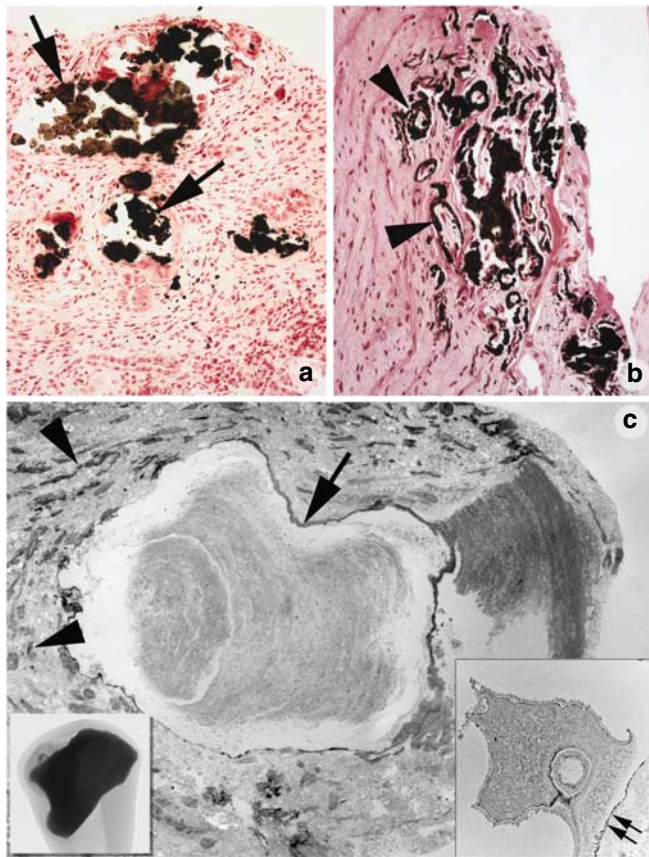
Figure 6 | Higher magnification reveals degree of cell loss and interstitial fibrosis. (**a**) Massive IMCD plugging (arrows) is associated with epithelial cell loss and severe fibrosis (patient 3). (**b**) Areas of abundant interstitial plaque (patient 2, arrowheads) were not associated with cell loss or interstitial fibrosis. (**c**) A large deposit in patient 1 (µCT in lower left inset) lies within an IMCD lumen (transmission electron microscopy, arrow); tubule cells are absent and crystals are apposed directly to the basement membrane (double arrow, detailed in lower right inset). Surrounding interstitium is fibrotic (arrowheads). Original magnification × 500 (**a**, **b**); × 1600 (**c**); and × 4800 (right lower inset).

Figure 7 | Mineral extends into the outer medulla and cortex in patients 1, 4, and 5. Yasue-positive deposits were found in outer medullary collecting ducts (**a**, arrows) and in the cortical collecting ducts (**b**, arrow) of patient 5; the same changes in patients 1 and 4 are not illustrated. Original magnification × 300 (**a**) and × 200 (**b**).

Figure 8 | Micro-Fourier-transform infrared spectrometer analysis of intra-luminal deposits and interstitial plaque from patient 3. Intra-luminal and interstitial crystals show a spectral band matching that of the hydroxyapatite standard, but no bands of the CaOx standard. Tissue with the embedding medium, a control, displays bands in common with neither standard.

DISCUSSION

All five of our patients exhibited the changes that were seen in patients with brushite stone, that is, IMCD and BD plugging with apatite crystals and loss of epithelial cell integrity, peritubular interstitial inflammation and fibrosis about the affected tubules; and papillary retraction and dilation of BD and their openings.[1] However, there are some differences. Only in patient 1 did we observe the extreme of BD dilation found regularly in brushite disease. Patients 2 and 3 had a larger fraction of IMCD involved than among the those with brushite stone that we have reported previously.[1] In contrast, our patients with dRTA had a very high fraction of IMCD involved with crystal plugging,[2] and somewhat less dramatic tubule dilation than that in patients with brushite stone. So one might say these five HPT patients share some traits of both brushite disease and dRTA. Likewise, patients with brushite stone had a very wide range of papillary involvement within individual patients, ranging from retraction and
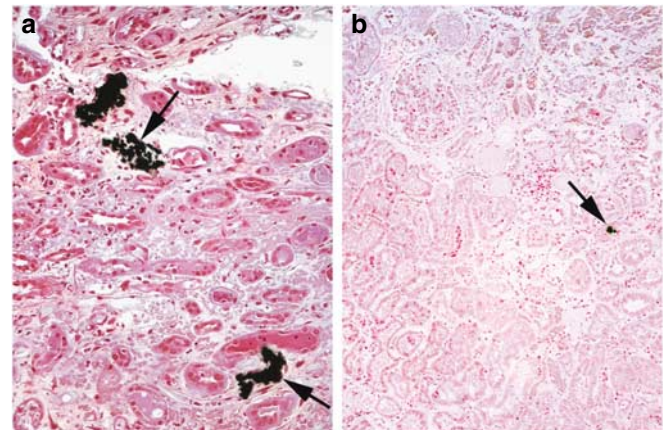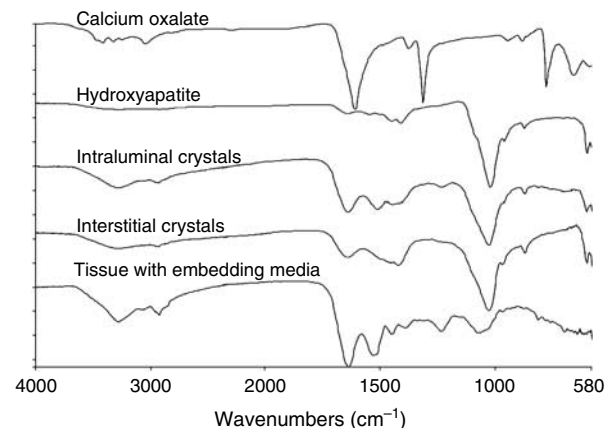
scarring to virtually normal, where in dRTA almost all papillae are quite abnormal; our HPT patients are more like those with brushite stone in having a wide range of changes. On the basis of the above distinctions, the findings from five HPT patients are similar to those from brushite disease and dRTA patients, but more closely resemble brushite disease than dRTA.

As patient 1 had only a net 33% of apatite in the stones that we had analyzed, she could have been classified clinically as having a CaOx stone. This finding from this one patient suggests that in HPT, unlike ICSF, CaOx stones may well be associated with the histopathology observed usually in patients with CaP stone. This conjecture cannot be tested until we biopsy more CaOx stone-containing patients with

HPT. One might mention in this regard that patients with CaOx stone who have enteric hyperoxaluria have thus far also showed presence of IMCD plugging with apatite, and are the only other instances of the presence CaOx stones with any crystals in their epithelial cell compartments.[3]

Unlike all four prior contrast groups with IMCD crystal plugging, patients with brushite stone, enteric hyperoxaluria with CaOx stones, dRTA, and cystinuria, these HPT patients can have some of their stones attached to Randall's plaque (patients 2 and 3). That they can have abundant plaque is not surprising in that hypercalciuria is well known in HPT[10] and a main pathophysiological correlate of plaque abundance.[9] Patient 2 was in fact hypercalciuric (Table 2), and plaque abundance was highest in patients 2 and 3 who had attached stones. For reasons yet to be uncovered, HPT can produce both pathologies: intratubular plugging and stone overgrowth on plaque, whereas no other disease yet described has them in combination. We could speculate that urine pH and volume, the other two factors controlling plaque abundance,[9] permit plaque in HPT and not in the other conditions involving IMCD plugging; this study cannot discuss this matter further due to lack of sufficient pre-parathyroidectomy urine studies.

Our published reports have thus far included 10 patients with brushite and 5 with dRTA stone.[1,2] In our publications, we did not chose to quantify whether stones were or were not attached, although this was fully documented at the time of our intraoperative observations. Among 82 fully studied papillae from the 10 patients with brushite stone, we found 22 stones excluding the index stones that led to the surgery. Of these, none were attached to plaque, but were rather suburothelial or attached to plugs of crystal growing out of the mouths of dilated BD. No stones were found attached to the papillae of our 5 dRTA patients, our 5 patients with cystine stone,[4] or our 4 patients with obesity bypass stone,[3] all of whom manifested IMCD apatite plugging. We offer these observations to put the present results in as quantitative a perspective as possible at this time.

Why IMCD plugging occurs in our HPT patients is an unsettled matter. In patients with brushite stone, hypercalciuria is more marked and urine pH is higher than in patients CaOx stone;[11] so supersaturation CaP is increased markedly and would be expected to foster CaP crystallizations in urine and IMCD and BD. The same is true for dRTA. We presume that both factors (high urine pH and calcium) were present in these HPT patients, but did not have the opportunity to study them before curative surgery. Postoperative recordings need not reflect those when HPT was present. More studies of HPT are clearly needed.

We have found virtually no prior information about renal tissue changes in primary HPT in patients who have stones; PubMed searches in fact revealed only three publications on the subject, and only when we relaxed the demand for stone formation. All the three publications describe patients with extreme hypercalcemia.[12–14] Changes included calcifications in glomeruli, mitochondria, and numerous tubular segments.

Serum calcium values ranged from 16 to 22 mg per 100 ml, far exceeding those of our patients.

MATERIALS AND METHODS
Patients
We studied five patients with primary HPT stone who required percutaneous nephrolithotomy at this institution (International Kidney Stone Institute, Methodist Clarian Hospital, Indianapolis, IN, USA) during the past 5 years (Table 1) and who consented to participate in the study. Patients were not selected. Clinical history was obtained along with reviews of old records to obtain stone analysis and the type and number of stone procedures (Table 1).

Clinical laboratory studies
Two 24-h urine samples were collected while patients were on their free-choice diet and were not on medications. In the urine we measured volume, pH, level of calcium, oxalate, citrate, phosphate, uric acid, sodium, potassium, magnesium, sulfate, and ammonia, and calculated supersaturation with respect to CaOx, BR, and uric acid using methods detailed elsewhere.[11] Routine clinical blood measurements were made on blood samples obtained for clinical purposes.

Biopsy protocol and plaque area determination
During percutaneous nephrolithotomy, all papillae were digitally imaged as described elsewhere.[9] Biopsies were taken from one upper pole, inter-polar, and lower pole papillum, and from the cortex. Using intraoperative recordings,[1] total surface area of each papilla was measured, and one of us outlined the areas of white (Randall's) plaque as well as the entire papilla on one set of prints. The white plaque and total papillary areas were converted to numbers of pixels, yielding the ratio of plaque to total papillary pixels, or percent coverage with plaque. No biopsy site inspected intraoperatively displayed significant hemorrhage and no postoperative complications related to the biopsy procedures occurred in any patient. The study was approved by the Institutional Review Board Committee for Clarian Health Partners (no. 98-073).

Tissue analysis
General. Fifteen papillary and five cortical biopsies were studied using light and transmission electron microscopy. All biopsy (cortical and papillary) specimens were immersed in 5% paraformaldehyde in 0.1 mol/l phosphate buffer (pH 7.4).

Light microscopy. Papillary and cortical biopsies were dehydrated through a series of graded ethanol concentrations to 100% ethanol prior to being embedded in a 50/50 mixture of Paraplast Xtra (Fisher Scientific, Itasca, IL, USA) and Peel-away Micro-Cut (Polysciences Inc., Warrington, PA, USA). Serial sections were cut at 4 μm and stained by Yasue metal substitution method for calcium histochemistry,[3] and hematoxylin and eosin for routine histological examination. An additional set of serial sections was cut at 7 μm for infrared analysis.

Infrared. Reflectance–absorption spectra were collected with a Perkin-Elmer Spotlight 400 infrared imaging microscope interfaced to a Perkin-Elmer Spectrum One Fourier transform infrared spectrometer. The system uses a 100×100 μm, liquid nitrogen-cooled, mercury cadmium telluride (HgCdTe) detector. Samples were analyzed using an aperture size suitable for the size of the sample being studied (for example, 50–20 μm in diameter). Each spectrum collected represents the average of 64 or 128 individual

scans having a spectral resolution of $4\,cm^{-1}$. A clean area on the low-E slide was employed to collect the background spectrum.

Attenuated total internal reflection spectra were collected with a Perkin-Elmer Spotlight 400 infrared imaging microscope interfaced to a Perkin-Elmer Spectrum One Fourier transform infrared spectrometer. The system uses a $100 \times 100\,\mu m$, liquid nitrogen-cooled, mercury cadmium telluride (HgCdTe) detector. The standard germanium internal reflection element was employed in conjunction with an aperture of $100 \times 100\,\mu m$ or $50 \times 50\,\mu m$. Since attenuated total internal reflection measurement is essentially an immersion measurement, the sampled area using these apertures is $25 \times 25\,\mu m$ or $12.5 \times 12.5\,\mu m$. Each spectrum collected represents the average of 64 or 128 individual scans having a spectral resolution of $4\,cm^{-1}$. A clean potassium chloride surface was used to collect the background spectrum.

Transmission electron microscopy. The 5-mm biopsy specimens of the renal papilla were divided into 1-mm blocks and routinely processed for transmission electron microscopy before being embedded.[3] All thin sections were examined with an FEI G2 Tecnai 12 BioTwin transmission electron microscope (FEI, Hillsboro, OR, USA), equipped with an AMT Corp., XR-60 Digital CCD system.

μCT. All papillary biopsies underwent μCT analysis with the SkyScan-1072 (Vluchtenburgstraat 3, B-2630 Aartselaar, Belgium) high-resolution desktop μCT system allowing nondestructive mapping of the location and size of the crystalline deposits within a biopsy specimen. This μCT system can generate a tissue window so that both the mineral deposit and tissue organization are seen at the same time. For this protocol, biopsies are quickly dipped in a 1:10 dilution of Hypaque (50%; Nycomed Inc., Princeton, NJ, USA)/phosphate-buffered saline, and then coated with a thin layer of paraffin and mounted in the center of a small chuck which is then locked into place in the machine. The sample was positioned in the center of the beam and the system configuration was set at 35 kV, 209 μA, 180° rotation, with flat-field correction. Images were recorded to CDs and reconstructed with Cone-Reconstruction software by SkyScan. These images were then reconstructed into three-dimensional images with SkyScan's CTAn + CTVol software. These images allowed us to properly orient each biopsy for future

light-microscopy analysis. Three separate scans from each patient were used to determine the number of sites of intraluminal deposits per square millimeter, except for patient 5 for whom paraffin sections were used.

REFERENCES
1. Evan AP, Lingeman JE, Coe FL *et al.* Crystal-associated nephropathy in patients with brushite nephrolithiasis. *Kidney Int* 2005; **67**: 576–591.
2. Evan AP, Lingeman J, Coe F *et al.* Renal histopathology of stone-forming patients with distal renal tubular acidosis. *Kidney Int* 2007; **71**: 795–801.
3. Evan AP, Lingeman JE, Coe FL *et al.* Randall's plaque of patients with nephrolithiasis begins in basement membranes of thin loops of Henle. *J Clin Invest* 2003; **111**: 607–616.
4. Evan AP, Coe FL, Lingeman JE *et al.* Renal crystal deposits and histopathology in patients with cystine stones. *Kidney Int* 2006; **69**: 2227–2235.
5. Matlaga BR, Coe FL, Evan AP *et al.* The role of Randall's plaques in the pathogenesis of calcium stones. *J Urol* 2007; **177**: 31–38.
6. Evan AP, Coe FL, Lingeman JE *et al.* Mechanism of formation of human calcium oxalate renal stones on Randall's plaque. *Anat Rec (Hoboken)* 2007; **290**: 1315–1323.
7. Odvina CV, Sakhaee K, Heller HJ *et al.* Biochemical characterization of primary hyperparathyroidism with and without kidney stones. *Urol Res* 2007; **35**: 123–128.
8. Pak CY, Poindexter JR, ms-Huet B *et al.* Predictive value of kidney stone composition in the detection of metabolic abnormalities. *Am J Med* 2003; **115**: 26–32.
9. Kuo RL, Lingeman JE, Evan AP *et al.* Urine calcium and volume predict coverage of renal papilla by Randall's plaque. *Kidney Int* 2003; **64**: 2150–2154.
10. Parks J, Coe F, Favus M. Hyperparathyroidism in nephrolithiasis. *Arch Intern Med* 1980; **140**: 1479–1481.
11. Parks JH, Worcester EM, Coe FL *et al.* Clinical implications of abundant calcium phosphate in routinely analyzed kidney stones. *Kidney Int* 2004; **66**: 777–785.
12. Henegar JR, Coleman JP, Cespedes J *et al.* Glomerular calcification in hypercalcemic nephropathy. *Arch Pathol Lab Med* 2003; **127**: E80–E85.
13. Kashitani T, Makino H, Nagake Y *et al.* Two cases of hypercalcemic nephropathy associated with primary hyperparathyroidism. *Nippon Jinzo Gakkai Shi* 1993; **35**: 1189–1194.
14. Yu JM, Pyo HJ, Choi DS *et al.* A case of primary hyperparathyroidism with hypercalcemic nephropathy in children. *J Korean Med Sci* 1994; **9**: 268–272.